



**Aerothermal Evaluation
of High-Temperature
Structural Materials for Use
in High-Performance Missile Design**

J. O. Ievalts and R. K. Matthews
ARO, Inc.

January 1980

Final Report for Period October 11 – 12, 1978

Approved for public release; distribution unlimited.

**ARNOLD ENGINEERING DEVELOPMENT CENTER
ARNOLD AIR FORCE STATION, TENNESSEE
AIR FORCE SYSTEMS COMMAND
UNITED STATES AIR FORCE**

NOTICES

When U. S. Government drawings, specifications, or other data are used for any purpose other than a definitely related Government procurement operation, the Government thereby incurs no responsibility nor any obligation whatsoever, and the fact that the Government may have formulated, furnished, or in any way supplied the said drawings, specifications, or other data, is not to be regarded by implication or otherwise, or in any manner licensing the holder or any other person or corporation, or conveying any rights or permission to manufacture, use, or sell any patented invention that may in any way be related thereto.

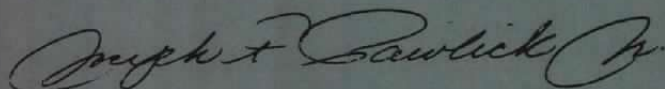
Qualified users may obtain copies of this report from the Defense Technical Information Center.

References to named commercial products in this report are not to be considered in any sense as an indorsement of the product by the United States Air Force or the Government.

This report has been reviewed by the Office of Public Affairs (PA) and is releasable to the National Technical Information Service (NTIS). At NTIS, it will be available to the general public, including foreign nations.

APPROVAL STATEMENT

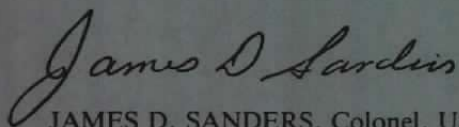
This report has been reviewed and approved.



JOSEPH F. PAWLICK, JR., Lt Colonel, USAF
Test Director, VKF Division
Directorate of Test Operations

Approval for publication:

FOR THE COMMANDER



JAMES D. SANDERS, Colonel, USAF
Deputy for Operations

UNCLASSIFIED

REPORT DOCUMENTATION PAGE		READ INSTRUCTIONS BEFORE COMPLETING FORM
1 REPORT NUMBER AEDC-TR-79-38	2 GOVT ACCESSION NO.	3 RECIPIENT'S CATALOG NUMBER
4 TITLE (and Subtitle) AEROTHERMAL EVALUATION OF HIGH-TEMPERATURE STRUCTURAL MATERIALS FOR USE IN HIGH- PERFORMANCE MISSILE DESIGN	5 TYPE OF REPORT & PERIOD COVERED Final Report - October 11-12, 1978	
	6 PERFORMING ORG. REPORT NUMBER	
7 AUTHOR(s) J. O. Ievalts and R. K. Matthews, ARO, Inc., a Sverdrup Corporation Company		8 CONTRACT OR GRANT NUMBER(s)
9 PERFORMING ORGANIZATION NAME AND ADDRESS Arnold Engineering Development Center/DOOV Air Force Systems Command Arnold Air Force Station, Tennessee 37389		10 PROGRAM ELEMENT, PROJECT, TASK AREA & WORK UNIT NUMBERS Program Element 62102F
11 CONTROLLING OFFICE NAME AND ADDRESS Air Force Materials Laboratory/MXE Wright-Patterson Air Force Base, Ohio 45433		12 REPORT DATE January 1980
		13 NUMBER OF PAGES 43
14 MONITORING AGENCY NAME & ADDRESS (if different from Controlling Office)		15 SECURITY CLASS (of this report) UNCLASSIFIED
		15a DECLASSIFICATION/DOWNGRADING SCHEDULE N/A
16 DISTRIBUTION STATEMENT (of this Report) Approved for public release, distribution unlimited.		
17 DISTRIBUTION STATEMENT (of the abstract entered in Block 20, if different from Report)		
18 SUPPLEMENTARY NOTES Available in Defense Technical Information Center (DTIC)		
19 KEY WORDS (Continue on reverse side if necessary and identify by block number) air to air missiles materials thermocouples flow fields short range (distance) polymers distribution hypersonic flow guided missiles metals heat transfer wind tunnel structural components panels shear stress tests		
20 ABSTRACT (Continue on reverse side if necessary and identify by block number) A materials screening test was conducted in the von Kármán Gas Dynamics Facility Wind Tunnel C to determine the performance of several high-temperature, polymeric and metallic composite materials being considered for use as missile structural components. Test conditions were representative of the aerothermal environment encountered during the projected flight of a high-performance, short-range air-to-air missile (SRAAM).		

UNCLASSIFIED

PREFACE

The work reported herein was conducted by the Arnold Engineering Development Center (AEDC) Air Force Systems Command (AFSC), at the request of the Air Force Materials Laboratory (AFML/MXE). The results of the tests were obtained by ARO, Inc. (a Sverdrup Corporation Company), contract operator of AEDC, AFSC, Arnold Air Force Station, Tennessee, under ARO Project Number V41C-W3. The AFML project manager was Mr. John Rhodehamel, who provided the material samples. Data reduction was completed on October 26, 1978, and the manuscript was submitted for publication on April 24, 1974.

CONTENTS

	<u>Page</u>
1.0 INTRODUCTION	5
2.0 APPARATUS	
2.1 Wind Tunnel	6
2.2 Test Hardware	6
2.3 Instrumentation	8
3.0 PROCEDURES	
3.1 Test Conditions	9
3.2 Test Procedures	9
3.3 Data Reduction	9
4.0 UNCERTAINTY OF DATA	
4.1 Test Conditions	11
4.2 Data	11
5.0 RESULTS AND DISCUSSION	
5.1 Test Environment	11
5.2 Test Results	13
6.0 CONCLUDING REMARKS	14
REFERENCES	15

ILLUSTRATIONS

Figure

1. Tunnel C	17
2. Sketch of Materials Testing Wedge	18
3. Sketch of Material Support Techniques	19
4. Curved-Surface Specimen Geometries	20
5. Sketch of Instrumented Wedge	21
6. Wedge Assembly in Tunnel C Test Section	22
7. Illustration of Typical Flight Environment	23
8. Sketch Illustrating Wedge Flow-Field Nomenclature	24
9. Illustration of Test Technique Used to Duplicate Flight Conditions	25
10. Summary of Flight Conditions Which Can Be Duplicated in AEDC-VKF Continuous Tunnels by Wedge Technique	26
11. Typical Shadowgraph Photograph	27

<u>Figure</u>	<u>Page</u>
12. Heat-Transfer and Shear Stress Distributions on Wedge Surface	28
13. Photographs of Curved-Surface Specimens During Run	29
14. Typical Curved-Surface Specimen Temperature-Time Histories	31
15. Posttest Photographs of Flat Panels	32
16. Typical Flat Panel Specimen Temperature-Time Histories	38

TABLES

1. Test Specimen Descriptions	39
2. Correlation of Specimen Numbering Schemes	40
3. Test Summary	41
 NOMENCLATURE	 42

1.0 INTRODUCTION

A materials screening test was conducted on high-temperature polymeric (polyimide) and Boron-Aluminum composite material specimens being considered for the next generation of short-range air-to-air missile (SRAAM) systems of the ILAAT* program. This work is part of a data generation effort initiated by the Air Force Materials Laboratory (AFML) and parallels work being done at the Tri-Service Thermal Flash Facility (AFML/MBC) and the Laser Hardened Materials Evaluation Laboratory (AFML/LPJ) at Wright-Patterson Air Force Base. Mission requirements for a typical short-range air-to-air missile (SRAAM) system call for Mach 4 flights lasting up to 20 sec. The objective of the present test, requested by the AFML, was to evaluate the performance of candidate materials in an aerothermal environment. However, this report is not intended to evaluate material performance or to make comparisons for the purpose of identifying "the best" material. That task is the responsibility of the AFML. This report presents the details of the test and the results.

Material samples prepared by the AFML were exposed to stagnation temperatures and local heating rates designed to simulate those encountered during a typical missile flight. The test specimens consisted of 51 material samples: 39 curved configurations of several radii and thicknesses and 12 flat panels. Both curved and flat panels were constructed from state-of-the-art materials provided by the AFML. These materials included panels of PMR-15, HR-600, and LARC polyimides reinforced with S-glass and/or Celion 6000 graphite. In addition, panels of aluminum reinforced with a boron-on-carbon core were tested under the same conditions. All samples were instrumented with thermocouples.

The tests were conducted in the AEDC von Kármán Gas Dynamics Facility (VKF), Hypersonic Wind Tunnel (C), which is a continuous-flow, Mach 10 wind tunnel. Test specimens were attached to a wedge model adapted to serve as a specimen holder. The desired flow conditions on the material sample were produced by adjusting the wedge angle. The oblique shock wave generated by the wedge was used to reduce the local Mach number on the wedge surface to the desired supersonic level ($M \approx 4$). The tunnel stagnation conditions were adjusted to produce the desired local pressure and temperature levels. Boundary-layer trips were positioned near the leading edge of the wedge to ensure a turbulent boundary layer. All of the runs were conducted at a nominal free-stream Mach number of 10, a flow total pressure of 1,220 psia, and a total temperature of 1,725°F.

*Inter-Laboratory-Air-to-Air-Technology.

Qualitative data on the material performance consisted of pretest and posttest photographs of the samples, 70-mm sequenced photographs, and 16-mm color motion pictures recorded during the test. In addition to the photographic data, heat-transfer-rate measurements were made to verify experimentally the predicted flow conditions; thermocouples were used to record material temperatures.

2.0 APPARATUS

2.1 WIND TUNNEL

Tunnel C (Fig. 1) is a closed-circuit, hypersonic wind tunnel with a Mach number 10, axisymmetric contoured nozzle, and a 50-in.-diam test section. The tunnel can be operated continuously over a range of pressure levels from 200 to 2,000 psia with air supplied by the AEDC-VKF main compressor plant. Stagnation temperatures sufficient to avoid air liquefaction in the test section (up to 1,800°F) are obtained through the use of a natural-gas-fired combustion heater in series with an electric resistance heater. The entire tunnel (throat, nozzle, test section, and diffuser) is cooled by integral, external water jackets. The tunnel is equipped with a model injection system, which allows removal of the model from the test section while the tunnel remains in operation. A more complete description of the tunnel may be found in Ref. 1.

The normal Mach 10 capabilities of Tunnel C were modified to meet the requirements of this test by means of a technique utilizing a large wedge to process the tunnel free-stream flow through an oblique shock wave. Varying the wedge angle and the tunnel free-stream conditions tailored the flow conditions on the surface of the wedge (where the material specimens were placed) to provide the needed test parameters. This test technique, developed at the AEDC-VKF specifically for materials testing (Ref. 2), makes it possible to use a hypersonic wind tunnel to simulate the aerodynamic convective heating rates and the total temperatures of supersonic flight environments.

2.2 TEST HARDWARE

The AEDC-VKF materials testing wedge (Fig. 2) was used to support the test specimens. The wedge is basically a 15-in. by 41.5-in.-long flat plate mounted on a 13-deg wedge block. The flat plate has a 1.5-in. back-step occurring 17.5 in. aft of the leading edge. Since the boundary layer on the flight vehicle would probably be turbulent, a turbulent boundary layer would be produced on the flat samples during the wind tunnel test. This was accomplished by spanning three rows of 0.078-in.-diam spheres across the wedge, 3 in. from

the leading edge. These spheres served to "trip" the boundary layer, causing the change from laminar to turbulent flow. A sketch of the trip sphere installation is also shown in Fig. 2.

A sketch illustrating how the 51 samples were installed on the wedge is presented in Fig. 3, and the geometries of the curved surfaces are shown in Fig. 4. The 39 curved surface specimens were bonded with RTV[®] to 15 square steel rods (0.625 in. square by 15.75 in. long) to provide a means of support during the test. All of the test specimens were instrumented with Chromel[®] -Alumel[®] (CR-AL) thermocouples to indicate the sample temperature-time histories. The thermocouple leads were attached to a 50-pin connector mated to a connector on the instrumentation cables. This was done to facilitate the interchange of specimens between runs.

Corresponding to the four geometries of the 39 curved segments were basically four types of materials (designated A, B, C, and D). The type A specimens were made from "addition" curing or polymerization of acetylene-modified polyimides, or those currently designated as the HR-600 (Thermid 600) series of oligomers. These specimens were reinforced with Celion 6000 woven graphite fabric. Types B and D were formed from polymerization of monomeric reactants (PMR) designated polyimides. The PMR polyimides result from a condensation-addition type of polymerization sequence. In the type B specimens, S-glass was employed as the reinforcement, whereas in the type D specimens, both S-glass and Celion 6000 graphite were used as reinforcement. Further, the D types were subjected to various processing pressure-temperature postcures. The projected use-temperature capabilities of the PMR-15 composite laminates were 600, 700, and 800°F. Type C specimens were prepared by pressure molding 6061 aluminum foils onto tapes of boron-on-carbon substrate reinforcement. A description of all specimens tested is presented in Table 1, and a list correlating the sample number with the rod or panel number is given in Table 2.

A steel "calibration plate" instrumented with heat-rate Gardon gages was installed to define the heating levels on the flat panels. It also provided a smooth, continuous surface in front of the curved-surface specimens. A sketch of the calibration plate showing the Gardon gage locations is presented in Fig. 5. Both the calibration plate and the flat panels were supported by phenolic spacers to ensure that the top surfaces of the samples or calibration plate were flush with the forward portion of the wedge (see Fig. 3).

The basic wedge angle was 13 deg; however, offset sting adapters were used in conjunction with the tunnel pitch mechanism to provide a wedge angle range from 0 to 28 deg. For the current test series the wedge angle was set at 21 deg. A photograph of the wedge assembly installed in the Tunnel C test section is shown in Fig. 6.

2.3 INSTRUMENTATION

The primary recorded data for this test consisted of 70-mm sequenced color photographs. A camera was installed to view the flat panels from the top of the tunnel, and the curved-surface samples were viewed from a camera mounted in the upstream side window. The cameras used Kodak® Varicolor II color film. The cameras were started at the beginning of each injection and were operated at a nominal rate of one frame per second.

In addition to the primary data, 16-mm color movies, videotape coverage, and 70-mm shadowgraph still photographs were also recorded. The movies were obtained with 16-mm motion picture cameras mounted adjacent to the sequenced cameras, loaded with Kodak VNF 7250 color film, and operated at 20 frames per second. Instant replay capability was provided by videotaping each run. This capability simplified decision making during the test by allowing each run to be reviewed immediately afterward. Two flow-field shadowgraph photographs were also obtained during each run by a single-pass, optical flow visualization system using Kodak Shellburst black-and-white film. In addition, pretest and posttest photographs of the test samples were obtained so that a good close-up comparison could be made of the samples before and after testing.

The photographic coverage provided good qualitative data; however, quantitative data were also desired. These were provided by CR-AL thermocouples attached to the material samples and by Gardon gages installed in the materials testing wedge assembly. The thermocouples were intended to measure "front" and "backside" temperature-time histories during each exposure. However, difficulties were experienced by the supplier during installation of the thermocouples, and, as a result, the precise depth locations of the thermocouples could not be determined. A thermocouple "bead" was formed using RTV® as the bonding agent to attach the bead to the surface. However, in many cases, the actual thermocouple junction did not appear to be on the material surface. This situation can produce temperature measurements that are significantly low; therefore, the higher temperature measurements are the most meaningful. The thermocouple output was digitized by a Beckman 210 analog-to-digital conversion system with each output scanned every 0.5 sec. The Gardon gages were used to measure the wedge surface heat-transfer rates. The location of the gages (see Fig. 5). provided for both axial and spanwise heating distributions. A description of these gages and their application is presented in Ref. 3. The gages were fabricated, calibrated, and installed by AEDC-VKF personnel.

3.0 PROCEDURES

3.1 TEST CONDITIONS

The nominal free-stream tunnel conditions are listed below.

<u>M_∞</u>	<u>P_o, psia</u>	<u>T_o, °F</u>	<u>H_o, Btu/lbm</u>
10.14	1,220	1,725	555

A complete test matrix showing the time of exposure for each panel and rod is presented in Table 3. A discussion of the local flow conditions on the wedge will be presented in a later section.

3.2 TEST PROCEDURES

Tunnel C uses a sting support mechanism that is retractable into an installation tank directly underneath the tunnel test section. The tank is separated from the tunnel by a pair of fairing doors and a safety door. When closed, the fairing doors, except for a slot for the pitch sector, cover the opening to the tank, and the safety door seals the tunnel from the tank area. After the model is prepared for a data run, the personnel access door to the installation tank is closed, the tank is vented to the tunnel flow, the safety and fairing doors are opened, and the model is injected into the airstream. After the data are recorded, the model is retracted into the tank, and the sequence is reversed with the tank vented to atmosphere to allow access to the model in preparation for the next run. This sequence is repeated for each configuration change.

Before injection into the tunnel flow, the wedge angle was set to 21 deg. This angle produced the desired flow conditions on the wedge surface. While the material specimens were in the tunnel, they were observed by means of a video monitor and by direct viewing through the tunnel side windows. If seriously damaged, the specimens were immediately removed from the flow by retracting the wedge assembly. Instrumentation outputs were recorded using the AEDC-VKF digital data scanner, beginning when the wedge reached the tunnel centerline and continuing until the wedge was retracted.

3.3 DATA REDUCTION

The primary data obtained in this test were the posttest conditions of the material samples themselves and the photographs of the samples documenting their performance

during the tunnel exposure. The tabulated data consist of tunnel parameters and model data; the model data were either (a) the temperature-time histories of the sample thermocouples or (b) the Gardon gage data from the wedge assembly.

The thermocouple readings were converted from millivolts to degrees Fahrenheit using least-squares polynomial curve fits of the data contained in Ref. 4.

The Gardon gages used in the wedge assembly are direct-reading heat-flux transducers whose output may be converted to heating rate (\dot{q}) by means of a laboratory-obtained calibration factor, i.e.,

$$\dot{q} = (CF)(\Delta E) \quad (1)$$

where ΔE is the gage millivolt output and CF is the gage calibration factor, Btu/ft²-sec/mv. The calibration factor for each gage was obtained by direct measurement of the gage output for a known radiant heating rate input. The calibrations were performed by personnel at AEDC.

The conversion from heating rate to heat-transfer coefficient (H_{T_o}) was accomplished by the relation

$$H_{T_o} \equiv \frac{\dot{q}}{T_o - T_w} \quad (2)$$

where T_o is the measured tunnel stagnation temperature* ($^{\circ}R$) and T_w is the effective wall temperature of the gage ($T_w = T_{GE} + 0.75 \Delta T$). The temperature adjustment for T_w accounts for the temperature gradient across the gage surface since the center of the sensing surface was slightly warmer than the outer case temperature (see Ref. 3 for discussion).

* The recovery temperature would ordinarily be used; however, since the determination of this parameter requires some assumptions, it has become common to substitute T_o (a measured parameter).

4.0 UNCERTAINTY OF DATA

4.1 TEST CONDITIONS

Uncertainties in the basic tunnel parameters were estimated from repeat calibrations of the P_o and T_o instruments and from the repeatability and uniformity of the tunnel flow during calibrations.

<u>Mach No.</u>	<u>Mach No.</u> <u>Nonuniformity</u>	<u>Uncertainty, percent(\pm)</u>	
		<u>P_o</u>	<u>T_o</u>
10.14	± 0.08	0.1	0.4

4.2 DATA

No uncertainty percentage can be established for the photographic data, but several pretest exposures of the test hardware in the tunnel were made to determine the optimum camera settings. The uncertainty of the heat-transfer-rate measurements is estimated to be ± 5 percent. The wall temperature measurements associated with each heat gage have an uncertainty of ± 0.5 percent of reading based on the wire manufacturer's specifications. Combination of these uncertainties results in an overall uncertainty in the heat-transfer coefficient of ± 6 percent. The temperature measurements on the material specimens are estimated to have an uncertainty of $\pm 4^\circ\text{F}$.

5.0 RESULTS AND DISCUSSION

5.1 TEST ENVIRONMENT

The use of a hypersonic wind tunnel to conduct tests requiring supersonic conditions is relatively new. As previously mentioned, this technique is described in Ref. 2, which emphasizes the importance of duplicating flight total temperature. Representative total temperatures encountered by typical missiles can clearly exceed $1,000^\circ\text{F}$, as is illustrated in Fig. 7. The fact that the Tunnel C heater can provide temperatures up to $1,800^\circ\text{F}$ is the primary reason why this facility can be used for this type of testing.

Figures 8 and 9 show the fundamentals of the test techniques used. The high total temperature hypersonic flow at Mach 10.14 was shocked down to a supersonic Mach number by the wedge, thereby providing local flow conditions on the wedge which duplicate the supersonic flight environment.

The use of a large wedge as a holder for material samples creates the two test regions illustrated in Fig. 8. Region I is limited in height by the distance of the bow shock above the wedge boundary layer at the aft end of the wedge. This distance is about 4.3 in. for the 41.5-in.-long wedge. Region I provided relatively uniform flow for testing the curved surface samples that were exposed to direct impact of the local flow. Much larger samples can be tested in Region II. (In fact, samples up to 25 in. long have recently been used.) In Region II, duplication of local shear stress, τ_L , is probably the most relevant parameter for the given total temperature level, T_o , whereas in Region I, duplication of total pressure, P_{oL} , total temperature, T_{oL} , and Mach number is of primary interest. This is accomplished, as illustrated in Fig. 9, by setting the proper tunnel stilling chamber conditions to simulate a given flight altitude. A summary of the supersonic flight conditions that can be duplicated in the AEDC-VKF hypersonic tunnels is presented in Fig. 10. This envelope can duplicate most of the operating envelopes of current aircraft and missiles. The application of this capability to the current test is illustrated in the following paragraphs.

The current test was conducted with $M_\infty = 10.14$ and with tunnel stilling chamber conditions (P_o and T_o) of 1,220 psia and 1,725°F (enthalpy was 555 Btu/lbm). The wedge angle was 21.0 deg; a shadowgraph picture, Fig. 11, shows the test regions previously discussed as well as the shock shape about a typical curved surface sample. After the air passed through the wedge-generated oblique shock, the calculated local Mach number on the wedge was 4.04. Since total enthalpy is conserved in crossing the shock, the local enthalpy downstream of the shock remains at 555 Btu/lbm. However, the total temperature increased to 1,735°F because of real-gas effects. The local total pressure was reduced to about 107 psia. It should be pointed out that these simple aerodynamic calculations, which can be found in Ref. 5, were modified slightly (<7%) by real-gas considerations. Now, with these calculated values for local Mach number (4.04), local total temperature (1,735°F), and local total pressure (107 psia), any of the remaining parameters of interest can be calculated.

For example, local static temperature (T_L) can be calculated as follows

$$T_L = \left(\frac{T_L}{T_\infty} \right)^* T_\infty \Rightarrow 87^\circ\text{F} \quad (3)$$

* From Ref. 5 for $M_\infty = 10.14$ and a wedge angle of 21.0 deg.

This static temperature is given in the MIL-STD-210B (Ref. 6) for hot-day operations at an altitude of about 6,600 ft. For the current test, simulation of the thermal environment at this relatively low altitude was of primary importance. It is unfortunate that current wind tunnel capabilities do not provide sufficiently high pressure levels to also simulate this *pressure* environment. The local static pressure (P_L) on the wedge is calculated as follows:

$$P_L = \left(\frac{P_L}{P_\infty} \right) P_\infty \Rightarrow 0.603 \text{ psia} \quad (4)$$

This static pressure exists in the atmosphere at an altitude of about 74,000 ft. The tunnel stilling chamber total temperature could have been reduced to simulate this altitude in terms of static temperature, also, but more importance was attached to the low-altitude (6,600-ft) thermal simulation.

In addition to the above calculations, some experimental measurements were also used to define the test conditions on the wedge surface. As mentioned in Section 2.2, these measurements were made with heat-transfer gages, and the results are presented in Fig. 12a in the form of heat-transfer coefficients. The data are compared to a theoretical heat-transfer prediction based on the method of Ref. 7. One of the primary conclusions illustrated by comparing these data to theory is the fact that the boundary-layer trips (see Fig. 5) were indeed effective in producing a turbulent boundary layer. A turbulent boundary-layer state is important because this is probably the state that would exist in actual flight.

The heat-transfer coefficients presented in Fig. 12a can be converted to local shear stress (τ_L) by the equation

$$\tau_L = H_{T_w} \frac{V_\delta}{c_p} \frac{1}{g_c} \quad (5)$$

where V_δ is the local inviscid wedge velocity, c_p is the specific heat of air, 0.24 Btu/lbm $^\circ$ R, and g_c is the gravitational constant, 32.174 ft-lbm/sec 2 -lbf. Shearing stress levels were about 2.5 lbf/ft 2 (Fig. 12b).

5.2 TEST RESULTS

This report is not intended to evaluate material performance or to identify "the best" material. The objectives are to present the testing techniques used and to present typical test results.

Typical photographs (Fig. 13) show the effect of the simulated Mach 4 environment on the curved panels. As can be clearly seen, all but one of the samples (Bc/Al) were glowing red-hot in the relatively short exposure times of 12 to 20 sec. In addition, the type A and type B samples exhibited some deterioration. The type C samples (Bc/Al) were the best conductors; as a result, heat was conducted away from the leading edge, a fact which probably explains why this sample does not appear to be significantly affected by the severe aerodynamic heating environment. The other types of materials are relatively good thermal insulators; as a result, the surface temperature rise is very rapid. However, the thermocouples that were intended to measure the sample temperature rise gave inconsistent results because of thermocouple junction attachment problems. Figure 14 presents the temperature-time histories measured by two of the thermocouples on the curved panels that may not have been affected by the attachment problems previously discussed. The thermocouple on the TRW-7A sample (type B) reached 800°F in about 16 sec. Since the local stagnation point recovery temperature for the simulated Mach 4 environment is about 1,560°F, the measured 800°F temperature is very reasonable. Because the curved panels are glowing red-hot, the *surface* temperatures in the stagnation region are probably significantly above 800°F.

Posttest photographs of the flat panels are presented in Fig. 15. The majority of these panels (9 of 12) survived the Mach 4 simulated environment with little or no degradation. The three panels that showed significant degradation (Figs. 15a, d, and g) appeared to delaminate due to local outgassing as surface bubbles (Fig. 15g). These grew to form a large bubble across the entire surface (Fig. 15a), finally leading to complete failure (Fig. 15d). The exposure times for the flat panels ranged from 22 to 35 sec. Figure 16 presents two typical temperature-time histories measured by representative thermocouples of the flat panels. The thermocouples on the flat panels reached about 400°F during a nominal 30-sec exposure. Again, thermocouple attachment problems were experienced; the data presented in Fig. 16 represent the highest recorded temperatures, which are believed to be the most meaningful.

6.0 CONCLUDING REMARKS

A materials screening test was conducted on candidate polyimide material specimens in a simulated Mach 4 environment. Fifty-one material samples were tested; 12 were configured as flat panels and 39 were curved surface samples. The local flow environment was produced by a wedge at a 21-deg angle in the Mach 10 hypersonic wind Tunnel C of the AEDC-VKF. The generated local flow conditions were Mach 4 with shear stresses of about 2.5 lbf/ft² and 1,735°F total temperature. The results of the test may be summarized as follows:

1. The use of a hypersonic wind tunnel to simulate the aerothermal environment encountered during supersonic flight ($M_\infty = 4$) has been demonstrated.
2. In general, the curved surfaces samples glowed red-hot and reached temperatures in excess of 800°F during an exposure time of about 15 seconds.
3. Nine of the twelve flat panel samples showed little or no degradation for exposure times of about 30 seconds.

REFERENCES

1. Sivells, J. C. "Aerodynamic Design and Calibration of the VKF 50-Inch Hypersonic Wind Tunnels." AEDC-TDR-62-230 (AD299774), March 1963.
2. Matthews, R. K. and Stallings, D. W. "Materials Testing in the VKF Continuous Flow Wind Tunnels." *Proceedings AIAA 9th Aerodynamic Testing Conference*. American Institute of Aeronautics and Astronautics, Inc., New York, 1976, pp. 233-237.
3. Trimmer, L. L., Matthews, R. K., and Buchanan, T. D. "Measurement of Aerodynamic Heat Rates at the von Kármán Facility." *ICIASF 1973 Record: International Congress of Instrumentation in Aerospace Simulation Facilities*. The Institute of Electrical and Electronic Engineers, New York, 1973, pp. 35-44.
4. Powell, Robert L., et. at. *Thermocouple Reference Tables Based on the IPTS-68*. National Bureau of Standards Monograph 125, Washington D.C., March 1974.
5. Ames Research Staff. *Equations, Tables, and Charts for Compressible Flow*. National Advisory Committee for Aeronautics (NACA) Report 1135, Washington, D.C. 1953.
6. Department of Defense. *Military Standard Climatic Extremes for Military Equipment*. MIL-STD-210B, Washington, D.C., December 1973.
7. Harms, Richard T., Schmidt, Craig M., Hanawalt, Arnold J., and Schmitt, Durwin A. *A Manual for Determining Aerodynamic Heating of High-Speed Aircraft*. Vol. 1. Report No. 7006-3352-001. Bell Aircraft Corporation, Buffalo, N.Y., 1959.

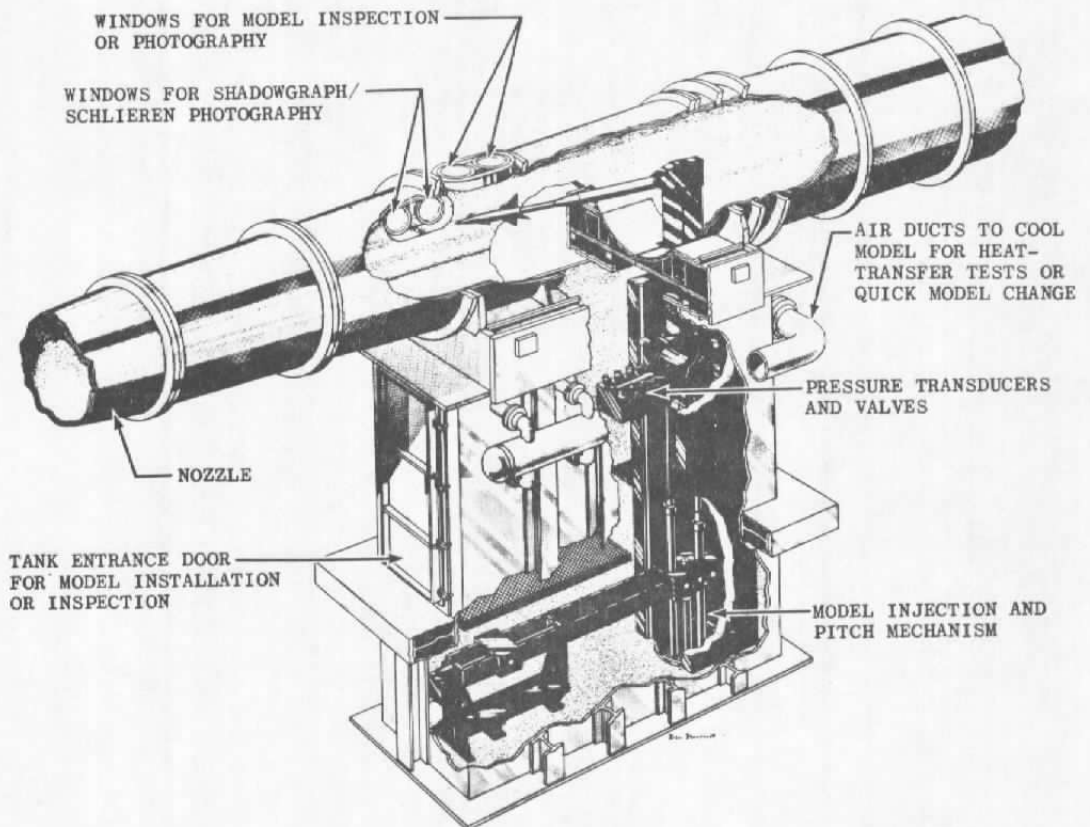
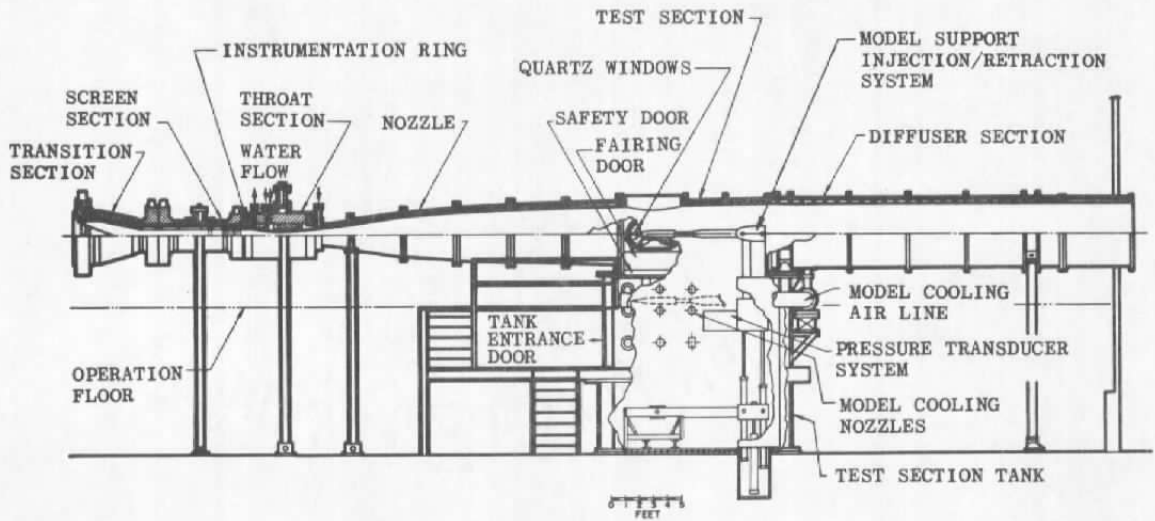
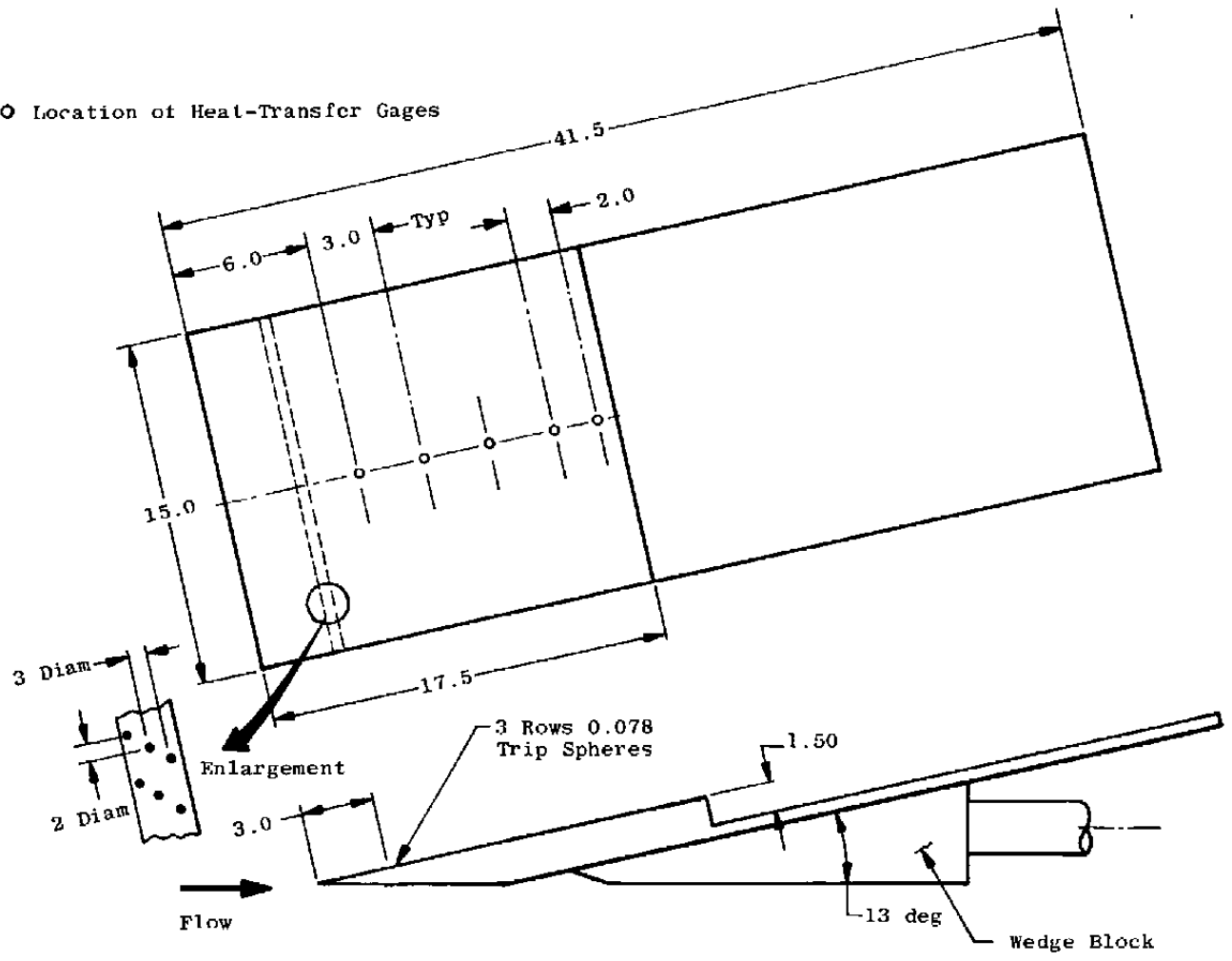


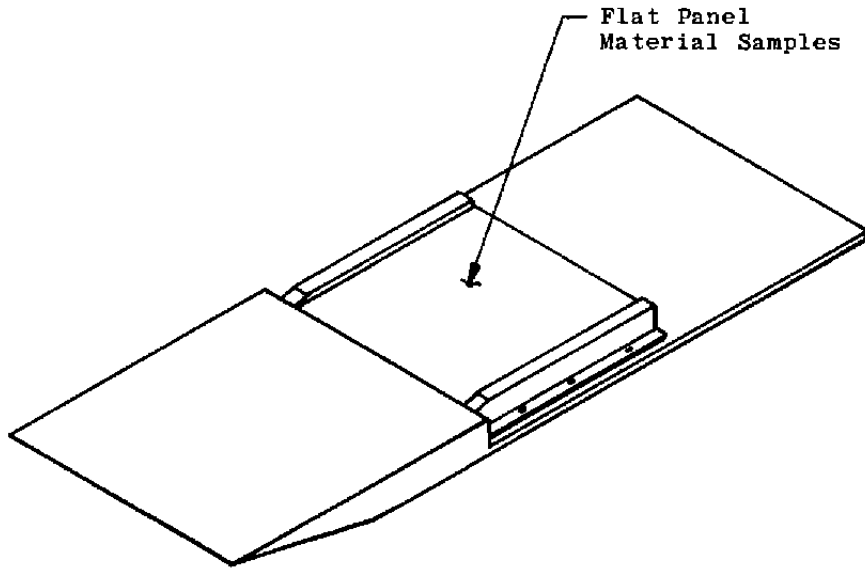
Figure 1. Tunnel C.

○ Location of Heat-Transfer Gages

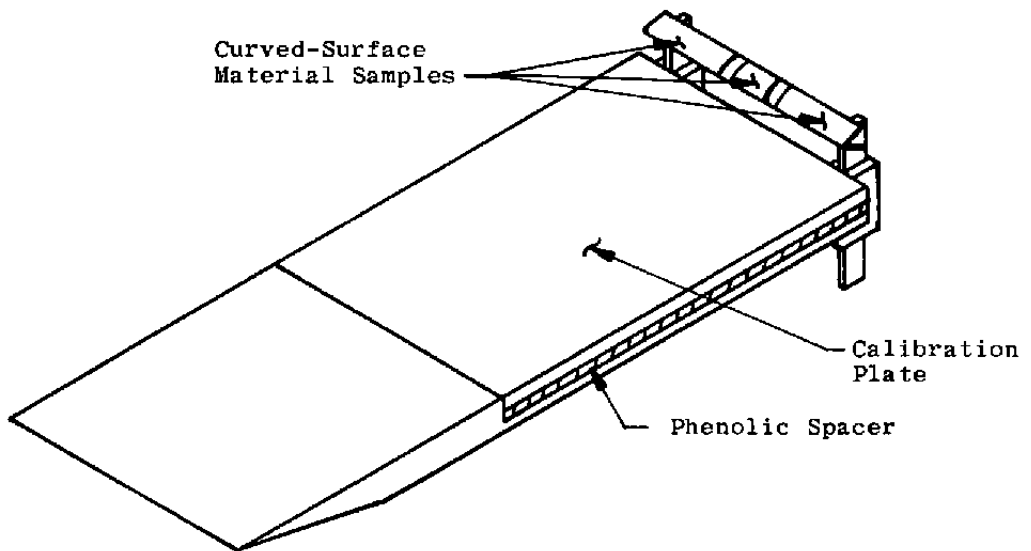


All Dimensions in Inches

Figure 2. Sketch of materials testing wedge.

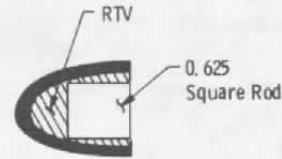


a. Flat panel specimens



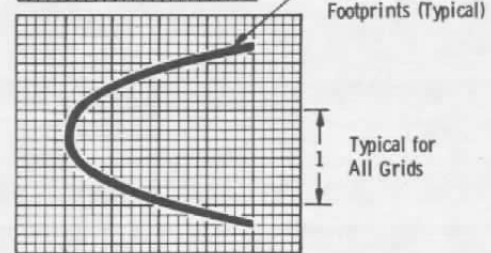
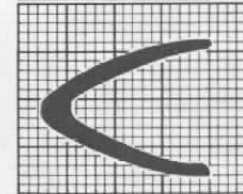
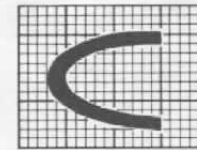
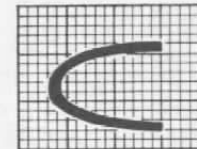
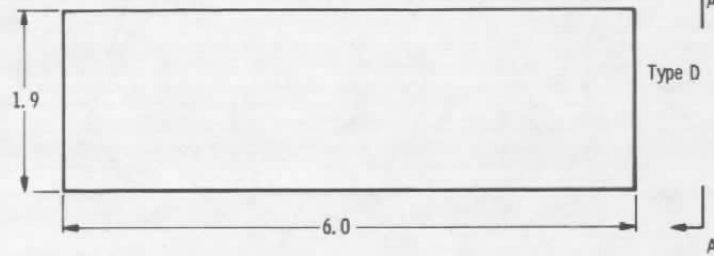
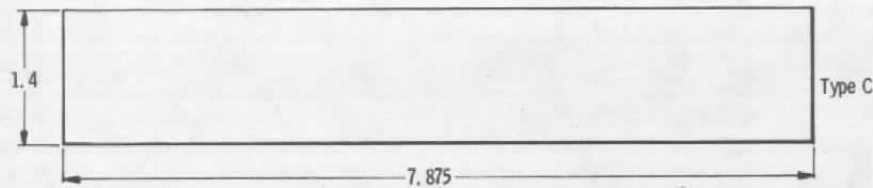
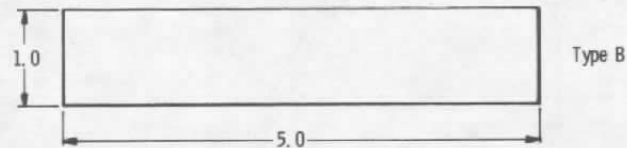
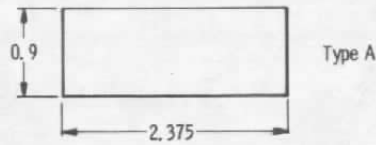
b. Curved-surface specimens

Figure 3. Sketch of material support techniques.



Typical Specimen Installation on Rod

All Dimensions in Inches



View A-A
(Typical for All Types)

Figure 4. Curved-surface specimen geometries.

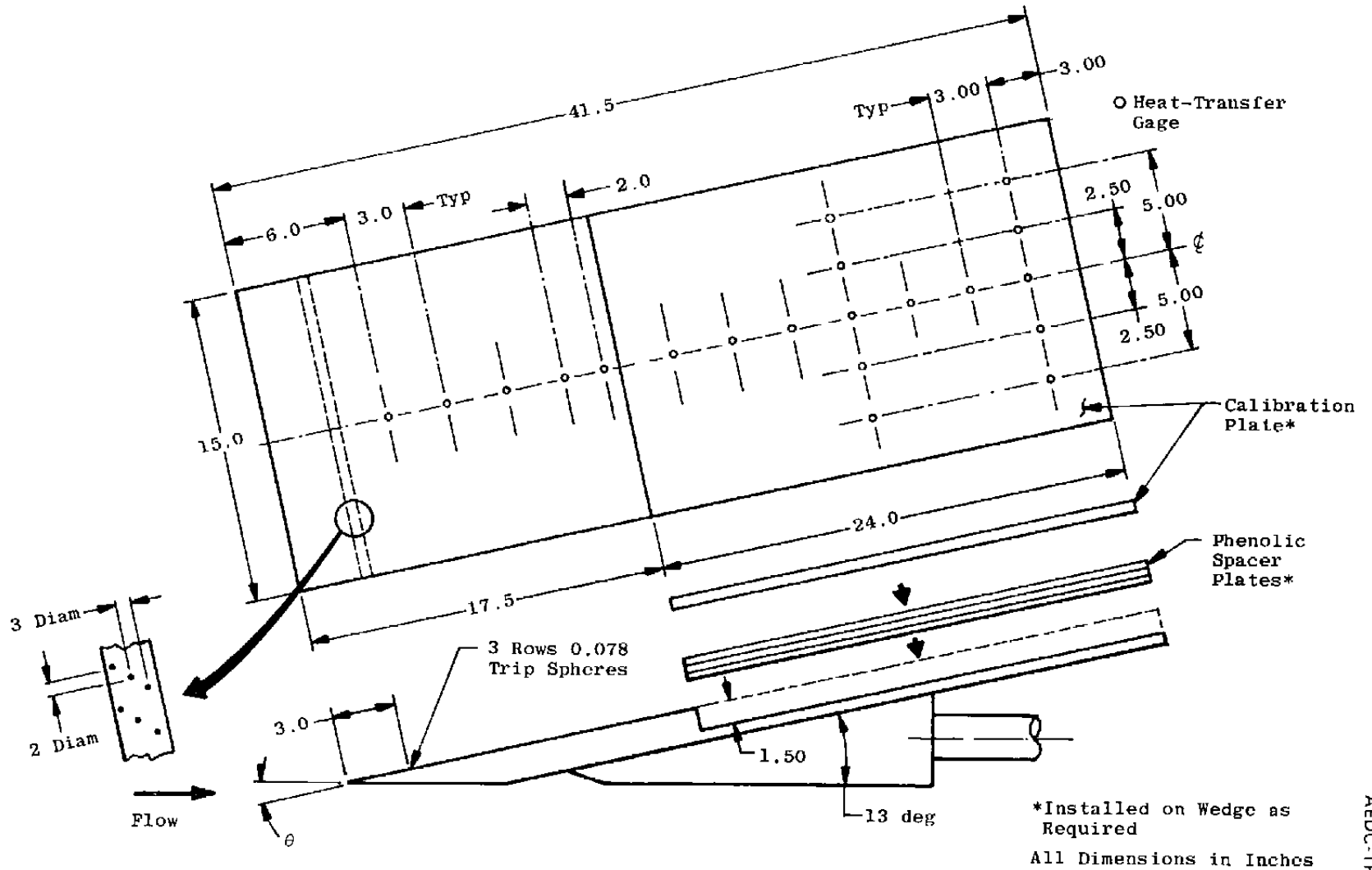


Figure 5. Sketch of instrumented wedge.

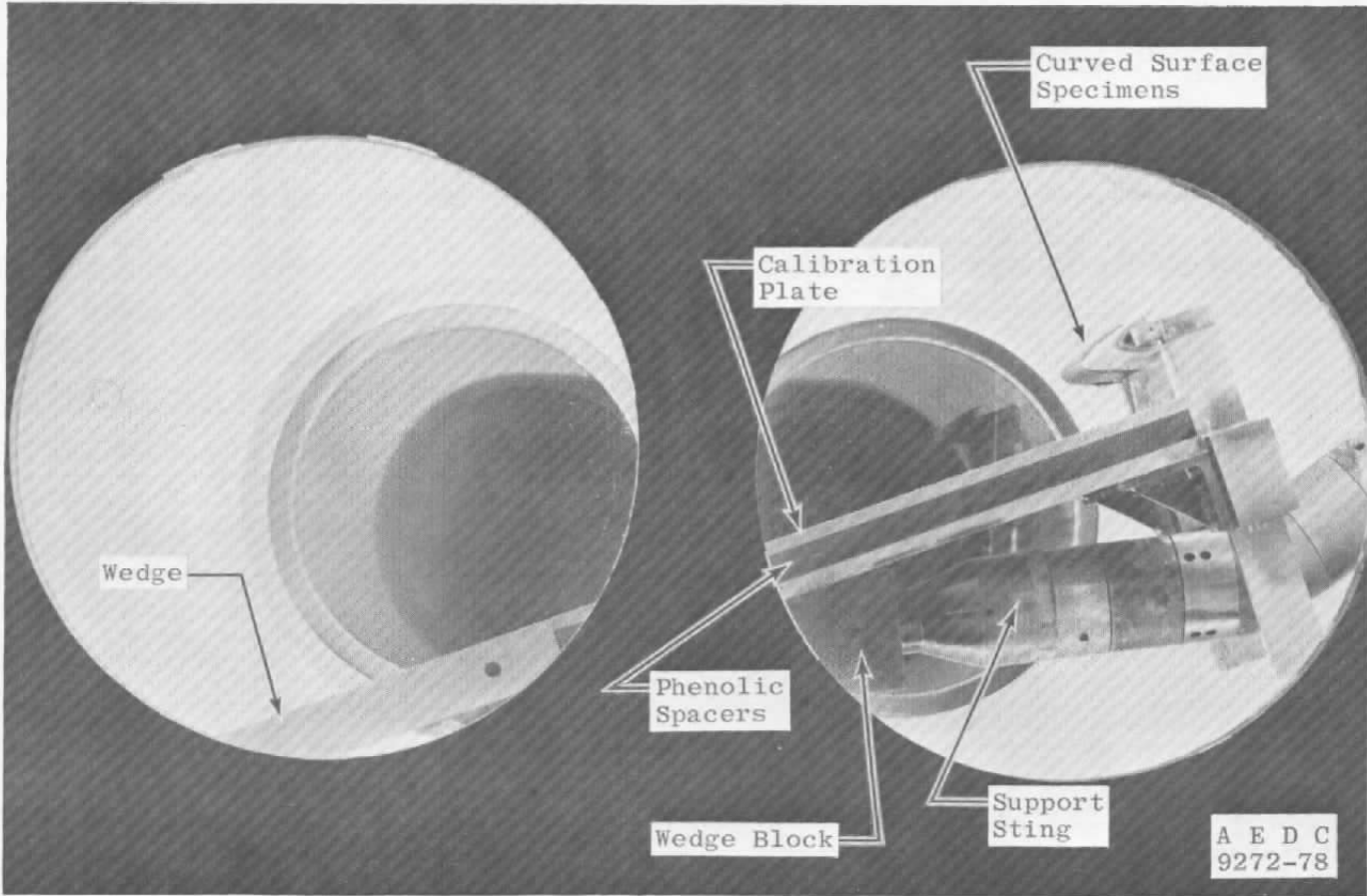


Figure 6. Wedge assembly in Tunnel C test section.

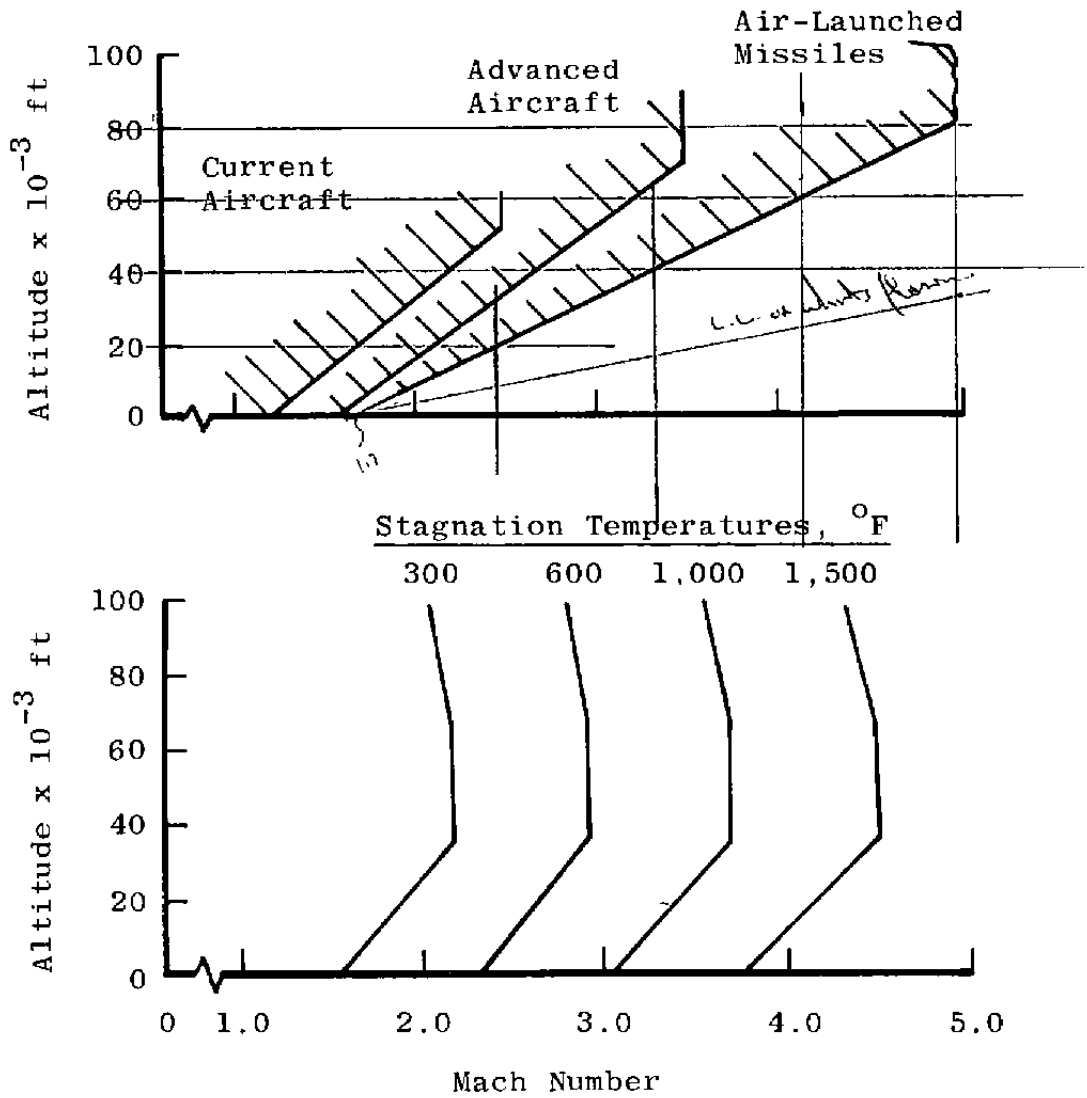


Figure 7. Illustration of typical flight environment.

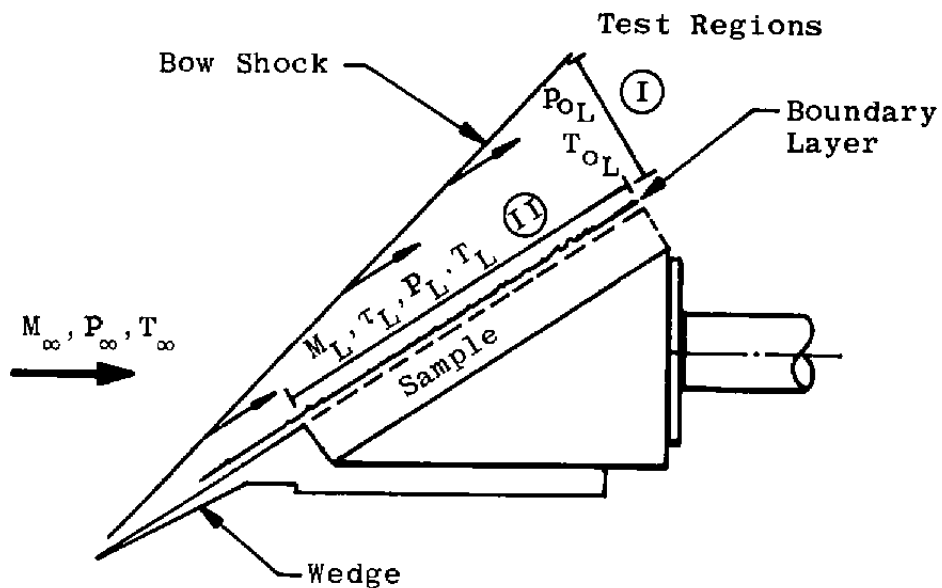
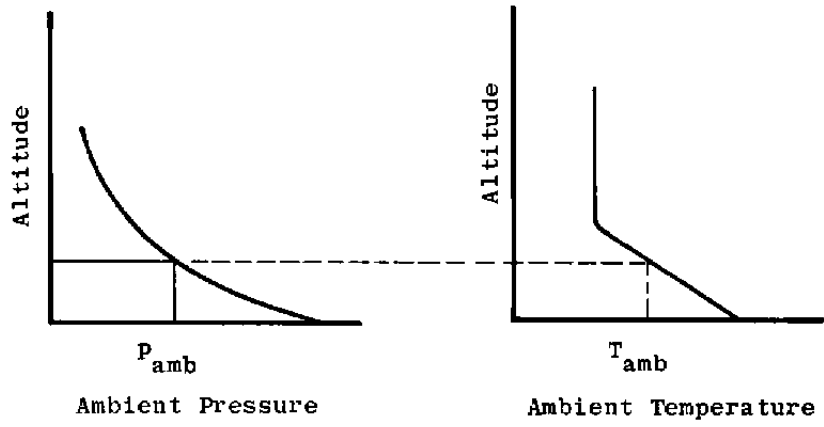


Figure 8. Sketch illustrating wedge flow-field nomenclature.



P_o , T_o , and θ can be adjusted such that:

 $P_L = P_{amb}$

 $T_L = T_{amb}$

 $M_L = M_{FLT}$

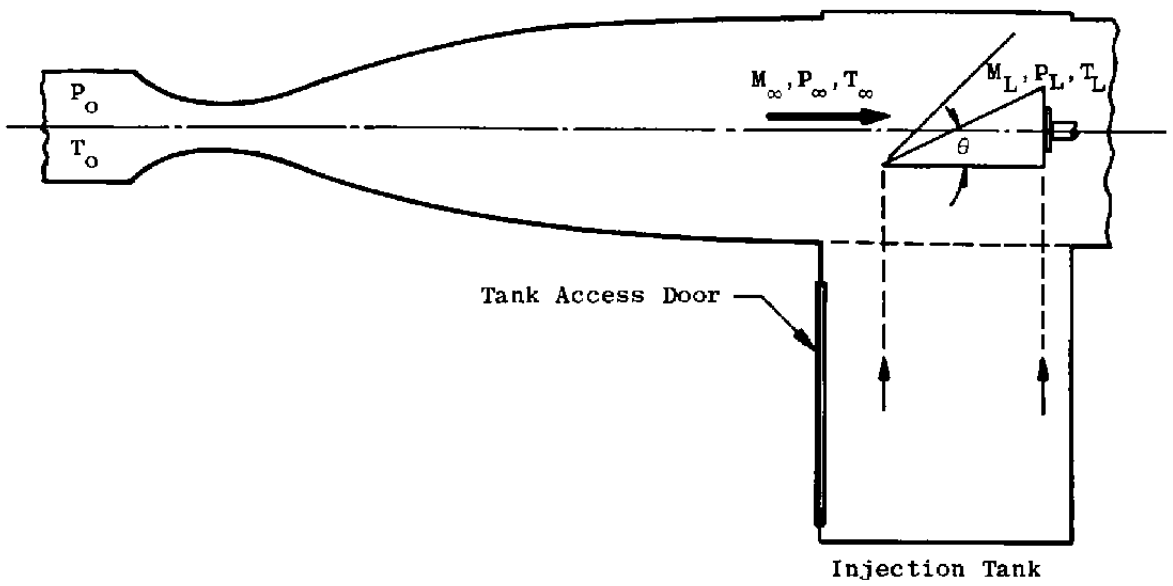


Figure 9. Illustration of test technique used to duplicate flight conditions.

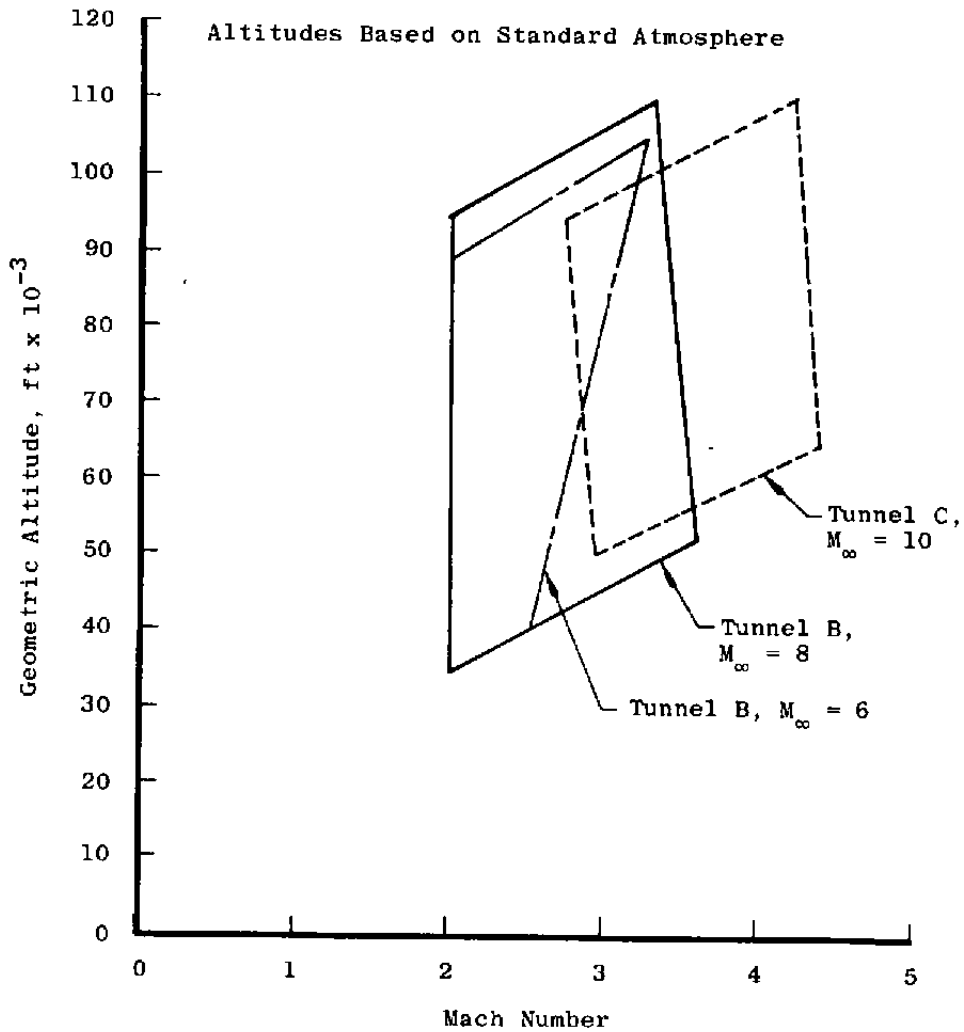


Figure 10. Summary of flight conditions which can be duplicated in AEDC-VKF continuous tunnels by wedge technique.

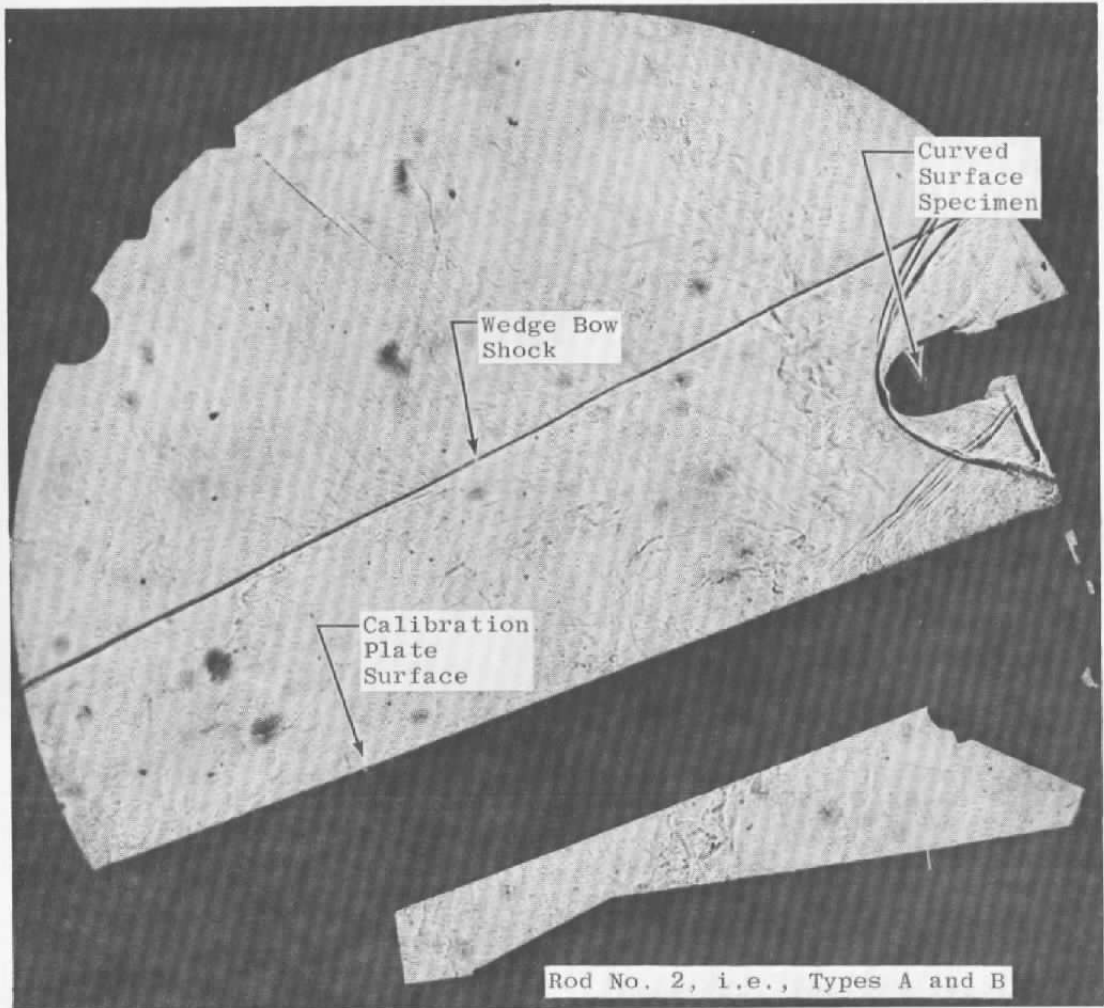
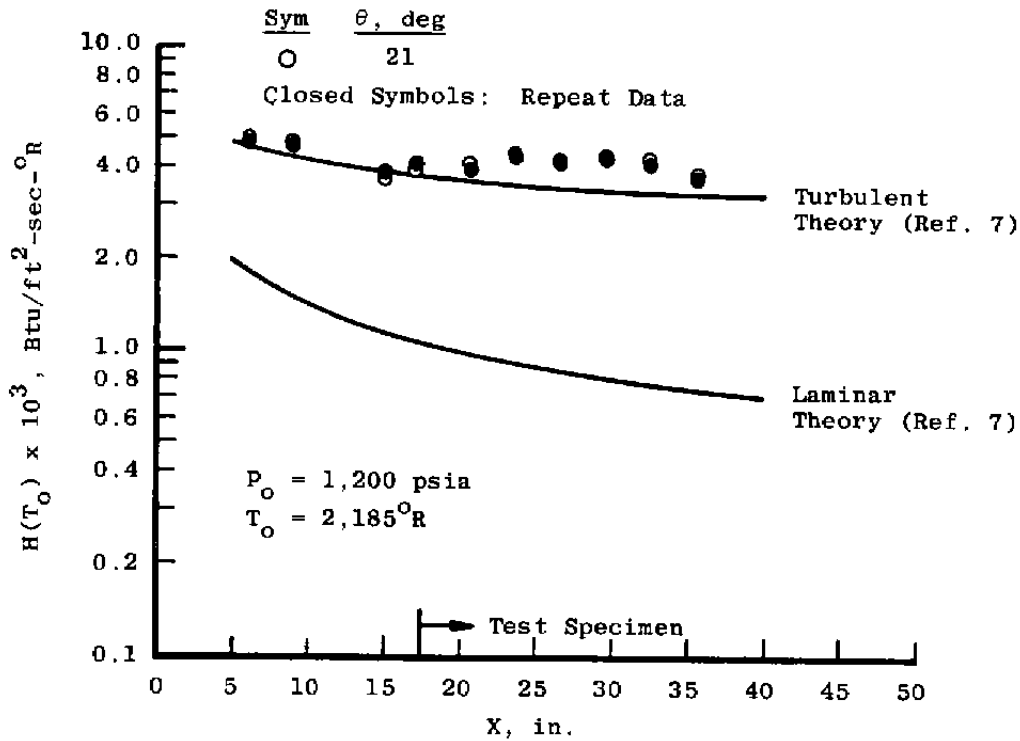
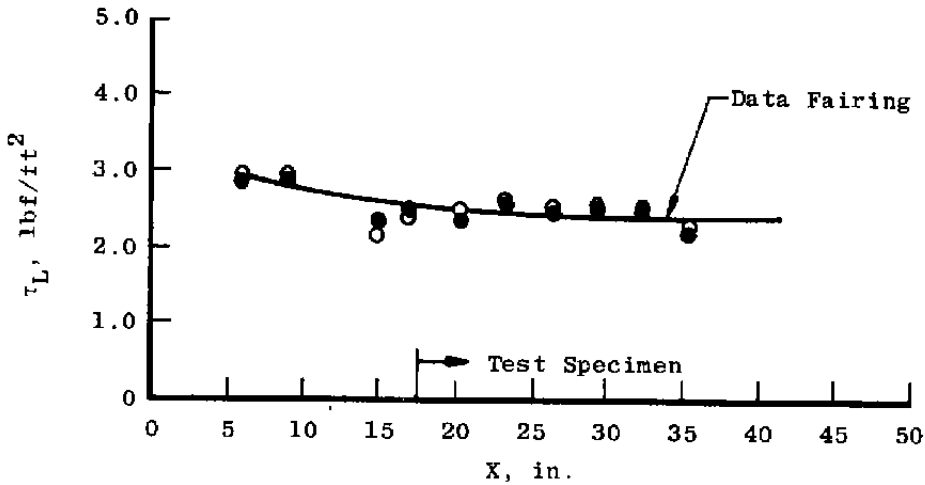


Figure 11. Typical shadowgraph photograph.



a. Heat-transfer distribution along centerline



b. Shear stress distribution along centerline

Figure 12. Heat-transfer and shear stress distributions on wedge surface.

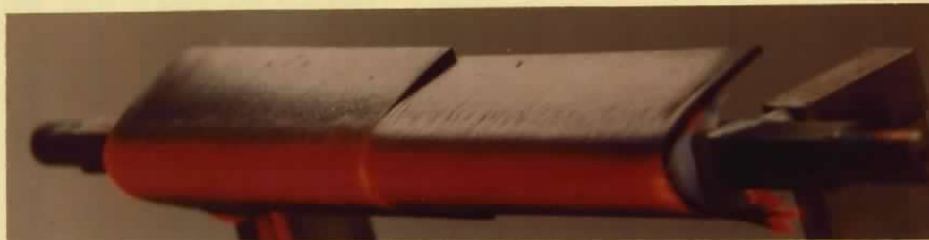
Time, sec

~20



Rod No. 6

~15



Rod No. 13

~12



Rod No. 2

~14



Rod No. 1

Figure 13. Photographs of curved-surface specimens during run.

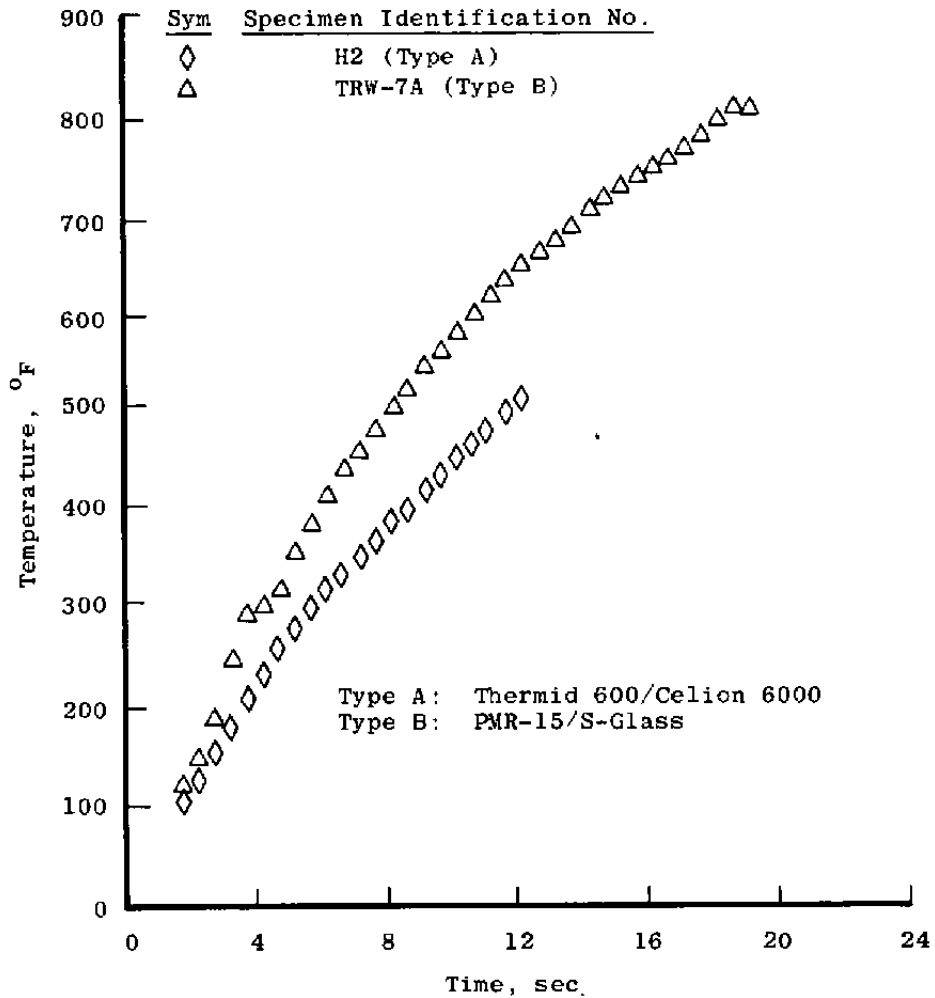
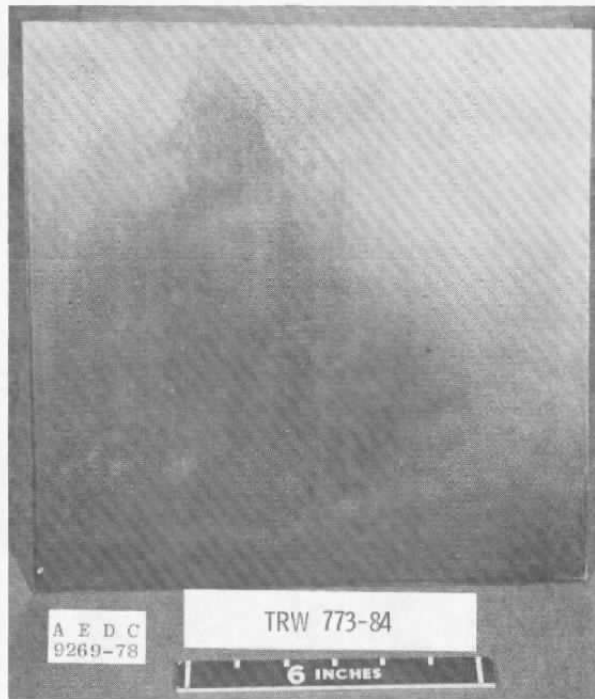


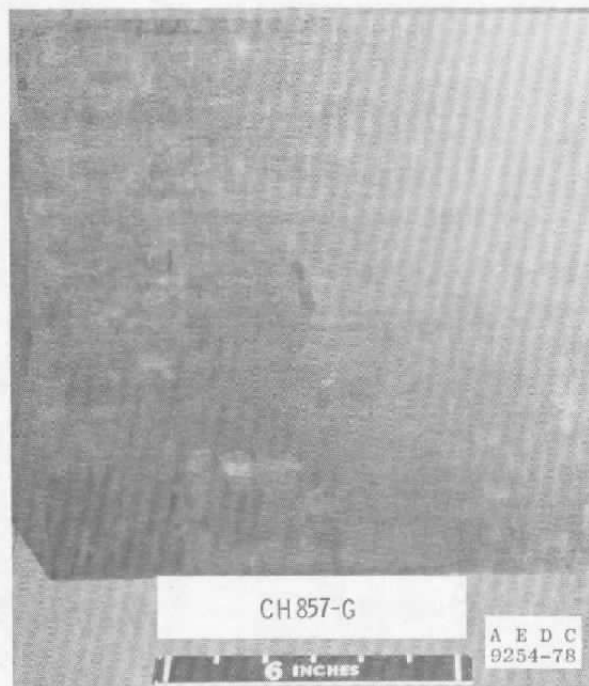
Figure 14. Typical curved-surface specimen temperature-time histories.



a. $t \approx 0.096$ in., total exposure time = 32.8 sec



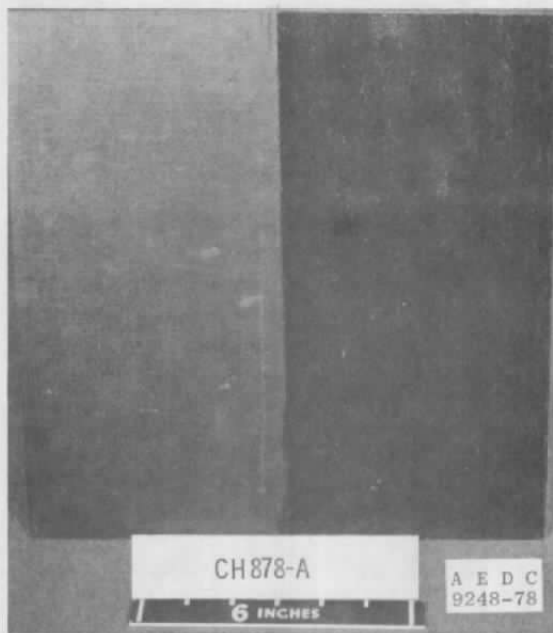
b. $t \approx 0.204$ in., total exposure time = 29.8 sec
Figure 15. Posttest photographs of flat panels.



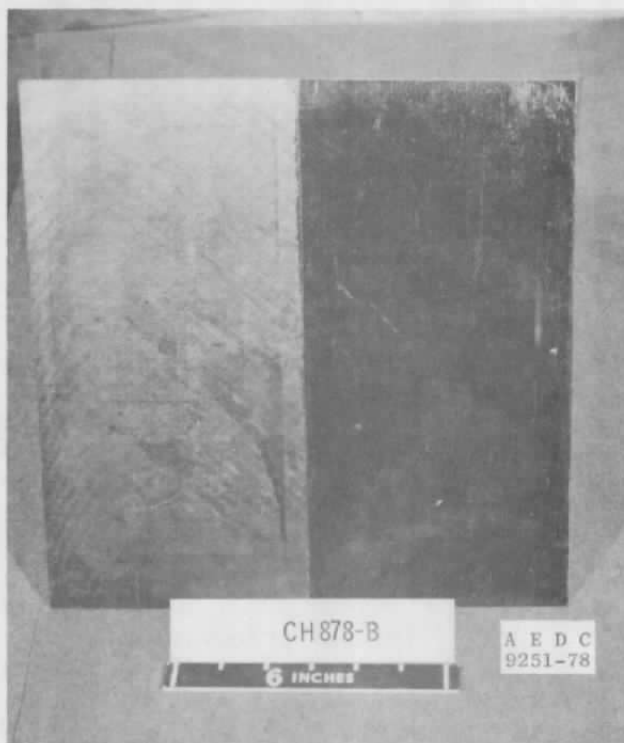
c. $t \approx 0.076$ in., total exposure time = 22.8 sec



d. $t \approx 0.112$ in., total exposure time = 33.3 sec
Figure 15. Continued.

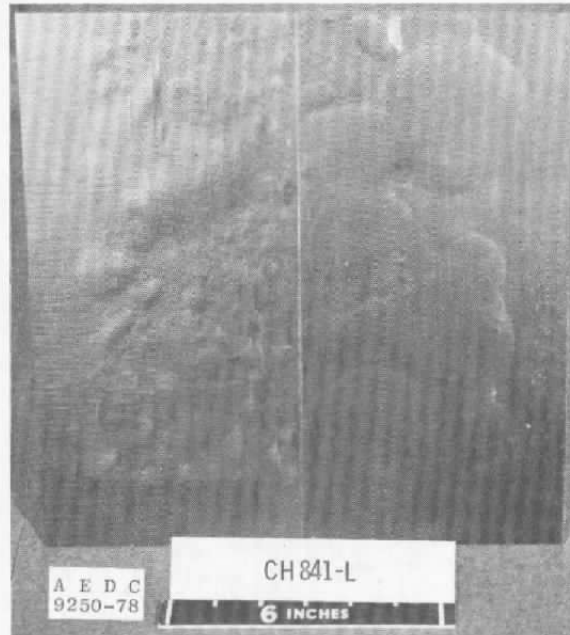


e. $t \approx 0.076$ in. (left), $t \approx 0.078$ in. (right), total exposure time for both = 30.3 sec

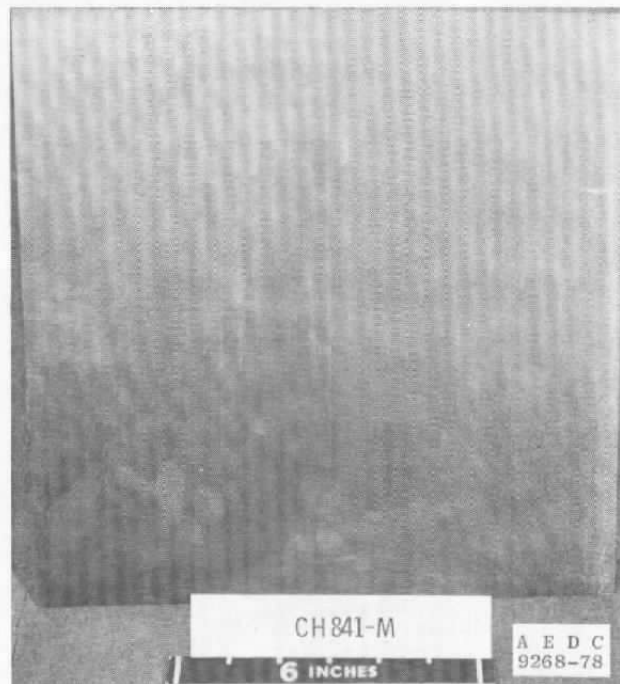


f. $t \approx 0.190$ in. (left), $t \approx 0.210$ in. (right), total exposure time for both = 31.3 sec

Figure 15. Continued.

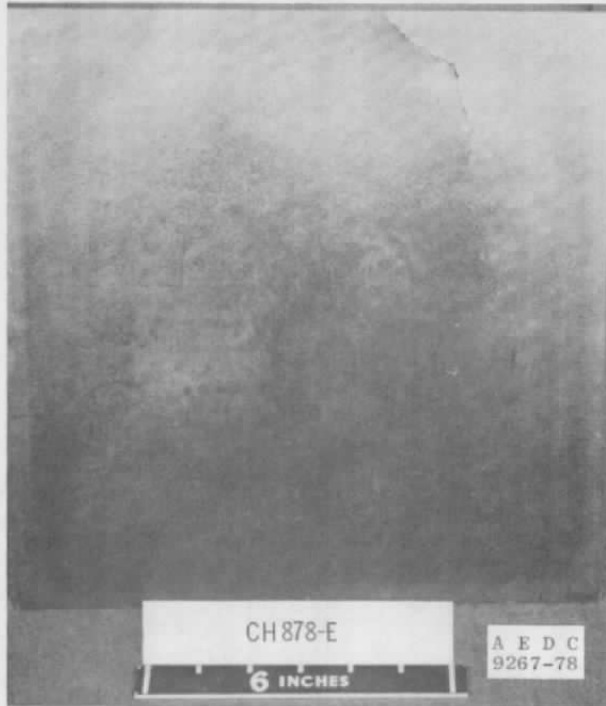


g. $t \approx 0.095$ in. (left), $t \approx 0.119$ in. (right), total exposure time for both = 33.8 sec

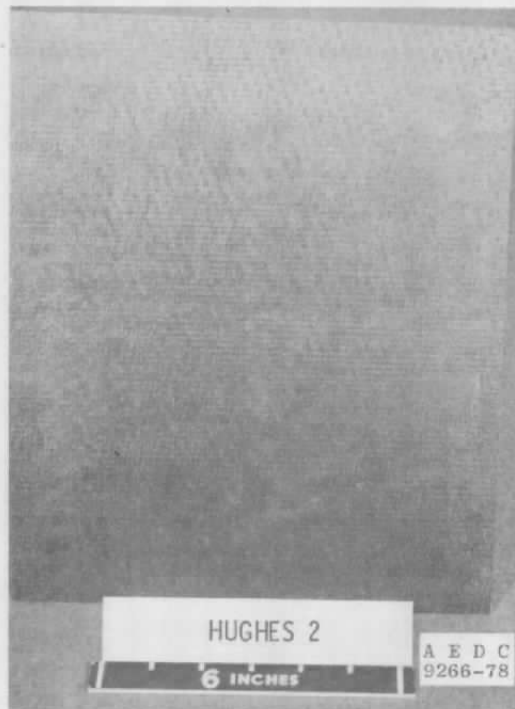


h. $t \approx 0.206$ in. (left), $t \approx 0.237$ in. (right), total exposure time for both = 34.3 sec

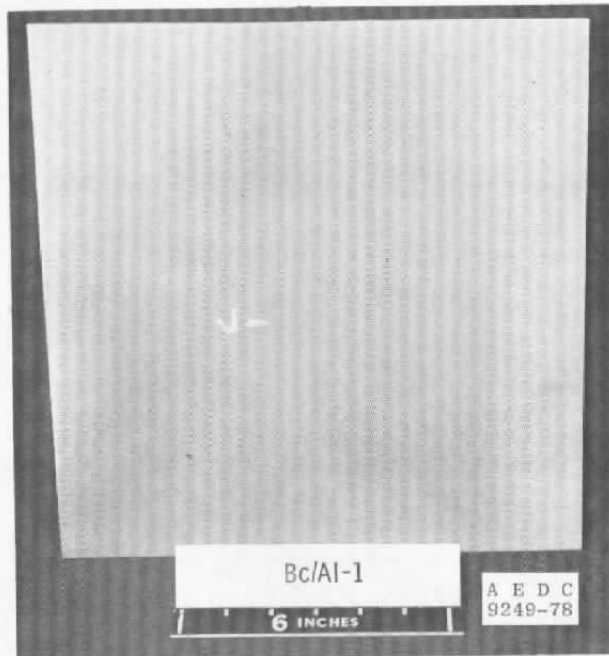
Figure 15. Continued.



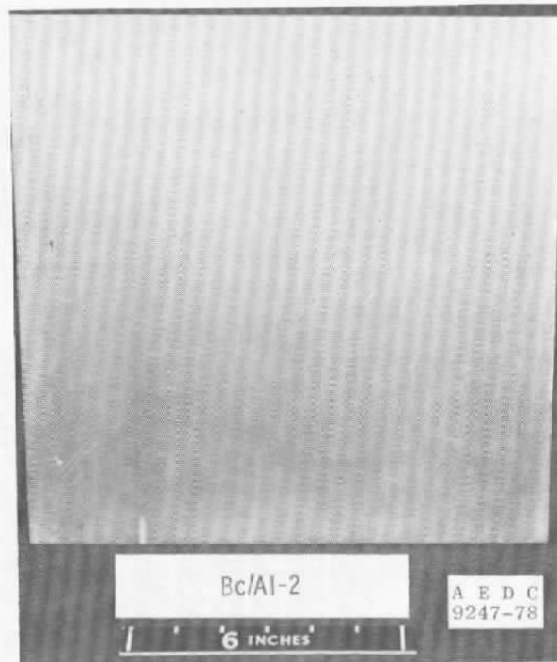
i. $t \approx 0.229$ in., total exposure time = 28.3 sec



j. $t \approx 0.139$ in., total exposure time = 35.3 sec
Figure 15. Continued.



k. $t \approx 0.045$ in., total exposure time = 29.3 sec



l. $t \approx 0.085$ in., total exposure time = 31.3 sec
Figure 15. Concluded.

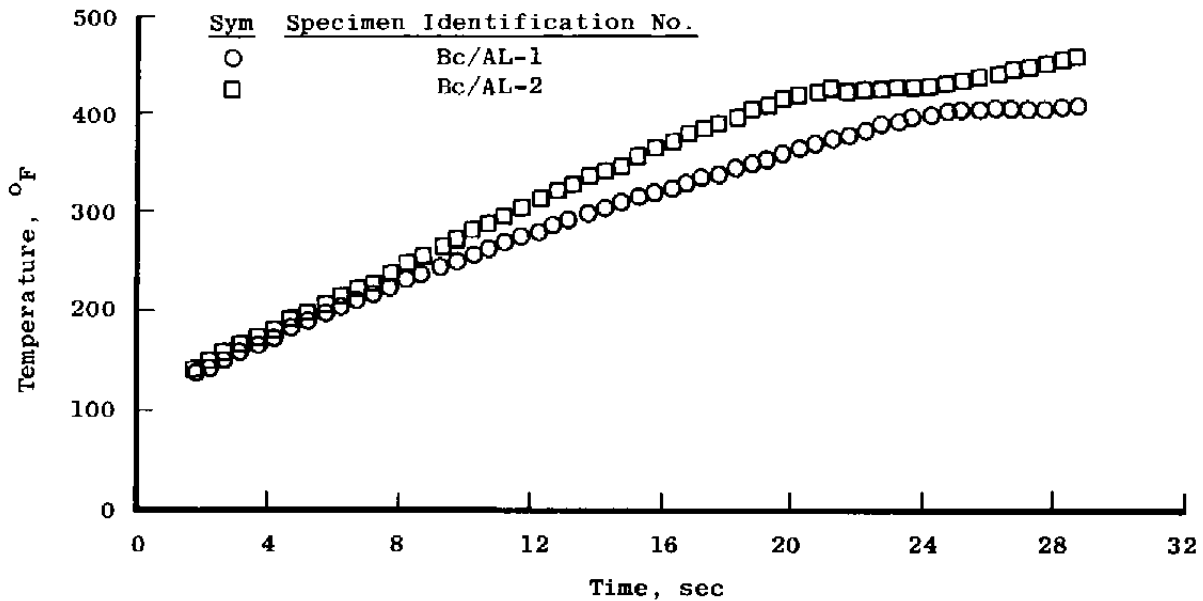


Figure 16. Typical flat panel specimen temperature-time histories.

Table 1. Test Specimen Descriptions

Specimen Identification Number	Resin/Matrix	Estimated Post-Cure Temperature, °F	Fiber Reinforcement	Coating	Thickness of Coating, in	Configuration Type	Sample Type	Panel Dimensions in.		
CH841-2A -2B -2C	PMR-15	600	Graphite Celion 6000	None	---	Curved Surface	D	N/A		
CH857-9A, -9B, -10A	PMR-15	800	Graphite Celion 6000	None	---	↓	D	↓		
CH878-9C, -10B, -10C	PMR-15	800	Graphite Celion 6000	NR-150B2	0.01		D			
CH841-JA, -JB, -JC	PMR-15	600	Graphite Celion 6000	S-Glass	0.02		D			
CH857-7A, -7B, -11A	PMR-15	700	S-Glass	None	---		D			
-11B, -11C, -12	"	"	"	"	---		"			
TRW-5A, -5B, -6A	PMR-15	600	S-Glass	None	---		B			
-7A -7B -8	"	"	"	"	---		"			
DWA-1 -2 -3 -4 -5 -6	6061 Aluminum	N/A	*	None	---		C			
H1 through H9	HR-600	N/A	Graphite Celion 6000	None	---		Curved Surface		A	N/A
TRW-773	PMR-15	N/A	S-Glass	None	---		Flat Panel		B	12 x 12 x 0.086
TRW-771-H4	PMR-15	N/A	S-Glass	None	---	↓	B	12 x 12 x 0.204		
CH857-G	PMR-15	800	Graphite Celion 6000	None	---		D	12 x 12 x 0.076		
CH857 I	PMR-15	800	Graphite Celion 6000	None	---		D	12 x 12 x 0.112		
CH878-A	PMR-15	800	Graphite Celion 6000	Half with NR-150B2	0.010 Nominal		D	12 x 12 x 0.076/0.078		
CH878 B	PMR-15	800	Graphite Celion 6000	Half with NR-150B2	0.01		D	12 x 12 x 0.190/0.210		
CH841-L	PMR-15	600	Graphite Celion 6000	Half with S-Glass	0.02		D	12 x 12 x 0.095/0.119		
CH841-M	PMR-15	600	Graphite Celion 6000	Half with S-Glass	0.02		D	12 x 12 x 0.206/0.237		
CH878-F	PMR-15	800	S-Glass	None	---		D	12 x 12 x 0.229		
Hughes 2	HR-600	N/A	Graphite Celion 6000	None	---		A	10 x 12 x 0.137		
Rc/AI-1	6061 Aluminum	N/A	*	None	---		Flat Panel	C	12 x 12 x 0.045	
Rc/AI-2	6061 Aluminum	N/A	*	None	---	L		12 x 12 x 0.085		

*Bolon-on-Carbon Substrate
 Note: N/A means not applicable

Table 2. Correlation of Specimen Numbering Schemes

Sample Number	Rod Number	Panel Number	Specimen Identification Number(s)	
1	1	N/A	CH841-3A, DWA-2	
2	2	↓	TRW-5A, H1, H2, TRW-5B	
3	3		CH857-7A, H6, TRW-8	
4	4		CH878-9C, H7, CH857-9A	
5	5		CH841-3B, H8, CH878-10B	
6	6		CH857-11C, H9, CH857-9B	
7	7		CH841-2A, DWA-4	
8	8		CH857-12, DWA-5	
9	9		CH878-10C, DWA-1	
10	10		CH857-10A, DWA-3	
11	11		CH841-2B, DWA-6	
12	12		CH857-7B, H3, TRW-6A	
13	13		CH841-3C, CH841-2C	
14	14		↓	CH857-11B, H4, TRW-7A
15	15		N/A	CH857-11A, H5, TRW-7B
16	N/A	1	CH857-G	
17	↓	2	Bc/A1-2	
18		3	TRW-773	
19		4	CH857-I	
20		5	Bc/A1-1	
21		6	CH878-A	
22		7	CH841-L	
23		8	CH878-B	
24		9	TRW-773-84	
25		10	CH841-M	
26		11	CH878-E	
27		N/A	12	Hughes 2

Notes: 1. Curved surface specimens are located on the rods in the order listed (left to right, locking downstream).

2. N/A means not applicable.

Table 3. Test Summary

Sample Number	M_L	T_{OL} , °F	τ_L , lbf/ft ²	Exposure Time, sec
1	4.04	1,735	N/A	17.8
2				11.8
2				12.8
3				12.8
4				22.3
5				17.3
6				20.3
7				6.3
8				13.8
8				39.5
9				21.3
10				22.3
11				8.3
12				17.3
13				17.3
14				21.3
15			N/A	16.8
16			2.5	22.8
17				31.3
18				22.8
19				33.3
20				29.3
21				30.3
22				33.8
23				31.3
24				29.8
25				34.3
26				28.3
27			2.5	35.3

NOMENCLATURE

CF	Gardon gage calibration factor, Btu/ft ² -sec/mv
c_p	Specific heat of air, Btu/lbm-°R
ΔE	Gardon gage electrical output, mv
g_c	Gravitational constant, 32.174 ft-lbm/sec ² -lbf
H_o	Total enthalpy based on T_o , Btu/lbm
H_{T_o}	Heat-transfer coefficient based on tunnel stilling chamber total temperature, Btu/ft ² -sec-°R
K	Gardon gage temperature calibration factor, °R/mv
M	Mach number
P	Pressure, psia
\dot{q}	Heating rate, Btu/ft ² -sec
T	Temperature, °R or °F as noted
ΔT	Temperature difference from Gardon gage center to edge, $\Delta T = (K)(\Delta E)$, °R
t	Nominal sample thickness, in.
V	Velocity, ft/sec
X	Distance from wedge leading edge, in.
θ	Wedge angle, deg
τ	Shear stress, lbf/ft ²

SUBSCRIPTS

amb	Ambient
FLT	Flight
GE	Gage edge

- L Local wedge surface conditions
- o Tunnel stilling chamber
- o_L Local total conditions
- w Gardon gage surface
- ∞ Free stream
- δ Inviscid wedge surface conditions